# Electromagnetic Analysis of Metal Braids

Harmen Schippers and Jaco Verpoorte
Avionics System Department
National Aerospace Laboratory NLR
Marknesse, The Netherlands
schipiw@nlr.nl

Ruben Otin
International Center for Numerical Methods in CIMNE
Barcelona, Spain
rotin@cimne.upc.edu

*Abstract*— **The shielding effectiveness of metal braids of cables is governed by the geometry and the materials of the braid. The shielding effectiveness can be characterised by the transfer impedance of the metal braid. Analytical models for the transfer impedance contain in general two components, one representing diffusion of electromagnetic energy through the metal braid, and a second part representing leakage of magnetic fields through the braid. The second part is a local phenomenon, which again has two parts: hole inductance and braid inductance. The paper will improved the analytical modelling of leakage of magnetic fields through the braid. Results of simulations are compared with measurements of several metal braids having different geometries.**

***Keywords-component; shielding effectivieness, transfer impedance, metal braid, inductance***

## I. INTRODUCTION )

The shielding effectiveness of metal braids of cables is governed by the geometry and the materials of the braid. A close-up of a typical metal braid is shown in Figure 1. The shielding effectiveness can be characterized by the transfer impedance of the metal braid. The transfer impedance can be calculated for a range of frequencies by appropriate analytical models or advanced numerical finite element models. The objective of this paper is to improve the analytical calculation of the transfer impedance of braided cable shields. Starting points are the analytical models of [1] and [2] and the semi-empirical models of [3]. The transfer impedance is used in the HIRF certification process to determine the common mode voltage in the cable due to the current flowing through the shield.

Figure 1 Close-up of metal braid

## II. DESCRIPION OF METAL BRAIDS

A metal braid is completely described by 6 parameters (see Figure 2 and Figure 3). These parameters are:

- Diameter D of braid (real number, dimension meters)
- Number of carriers C (i.e. belts of wires) in the braid (integer number)
- Number of wires N in a carrier (integer number)
- Diameter d of a single wire (real number, dimension meters)
- Conductivity $\sigma$ of the wires (real number, dimension S/m)
- Weave angle $\alpha$ of the braid (real number, degrees)

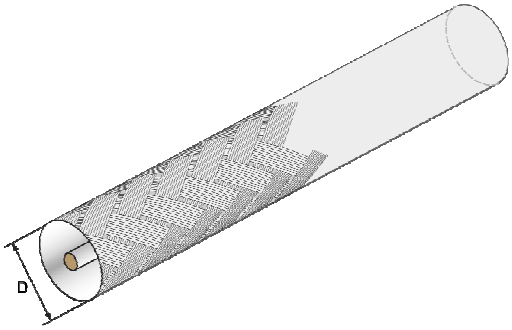


Figure 2 Metal braid for cable (diameter of braid is D)

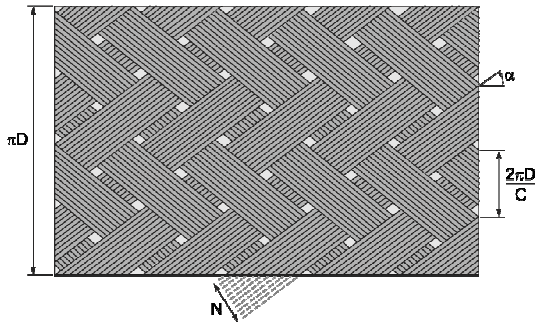


Figure 3 Characteristics of metal braid

## III. AVAILABLE ANALYTICAL MODELS

Analytical models for calculation of the transfer impedance contain in general two components, one part ( $Z_d$ ) representing diffusion of electromagnetic energy through the metal braid, and a second part ( $j\omega M$ ) representing leakage of magnetic fields through the braid

$$Z_t = Z_d + j\omega\upsilon M \qquad (1)$$

with $\upsilon$ the number of holes per unit length . The diffusion component $Z_d$ of the metal braid is governed by the DC resistance of the metal braid and diffusion of waves through the wall of the cylindrical braid. Following Ref [1] the diffusion can be computed by

$$Z_d = R_0 \frac{\gamma d}{\sinh \gamma d} \qquad (2)$$

where $d$ is the thickness of the wires in the metal braid, and $\gamma$ is the complex propagation constant of the wires ( $\gamma = (1+j)/\delta$ , with $\delta$ the skin depth of the wire, $\delta = \sqrt{2/\omega\mu\sigma}$ ). The resistance $R_0$ is computed per unit length. The DC resistance $R_0$ is governed by the conductivity $\sigma$ and the averaged cross section of the braid. With reference to [1] the resistance per unit length reads

$$R_0 = \frac{4}{\pi d^2 NC\sigma\cos(\alpha)} \qquad (3)$$

The second term of (1) is governed by the inductance of magnetic fields through the apertures in the metal braid. The inductance is a local phenomenon. Expressions for the inductance can be derived by considering the inductance through a single aperture and then superimposing the contributions of all apertures. Hence, the interaction of induced magnetic fields through neighboring apertures is usually neglected. In general, the inductance has two parts: hole inductance and braid inductance. The hole inductance $M_h$ is caused by penetration of magnetic fields through the rhombic apertures in the metal braid (see Figure 3), while the braid inductance $M_b$ arises from the woven nature of the braid. In the semi-empirical models as described by [3] a third inductance term is introduced, the skin inductance $M_s$, which is due to eddy current in the walls of the rhombic apertures. In summary, the inductance $M$ in equation (1) is the superposition of the hole inductance $M_h$ , braid inductance $M_b$ and skin inductance $M_s$ ,

$$M = M_h + M_b + M_s \qquad (4)$$

In the analytical model of Ref [1] only the hole inductance through the rhombic apertures of a thin braid is considered. Here, the braid inductance and skin inductance are neglected $M_b = M_s = 0$ .

The main improvement of the analytical models of Vance (see [1] and [2]) and the semi-empirical formulas of Kley [3] are discussed below. The detailed electromagnetic analysis of the formulas of Vance will provide a more correct model for the hole inductance term $M_h$ . The semi-empirical formulas of Kley are discussed with respect to analytical approaches as presented by Tyni [4]. The semi-empirical formulas of Kley were derived for a class of optimized single-braided cable shields by adjusting the parameters to measured data of a batch of samples. The formulas are approximations of the basic models of Tyni [4].

## IV. IMPROVEMENT OF HOLE INDUCTANCE

In Ref [1] the hole inductance is calculated by

$$M_h = \frac{\mu m}{2\pi^2 D^2} \qquad (5)$$

with $m$ the magnetic polarizability of one rhombic hole. This model has been adapted by Kley [3], where the thickness and the curvature of the braid are considered. Therefore, in Ref [3] the hole inductance is calculated by

$$M_h = 0.875 \frac{\mu m}{2\pi^2 D_m^2} e^{-\tau} \qquad (6)$$

The factor 0.875 in equation (6) takes into account the curvature of the braid. The outer diameter $D_m$ of the braid is approximated by $D_m = D + 2d$ . The effect of the wall thickness of the braid is taken into account by multiplying the right-hand side of (5) with an attenuation factor $\exp(-\tau)$ due the so-called “chimney” effect. Referring to [3] the factor $\tau$ in the exponent of (6) reads

$$\tau = 9.6F \sqrt[3]{F^2 (2-F)^2 d / D_m} \qquad (7)$$

where $F$ is the fill of the braid

$$F = \frac{NCd}{2\pi D_m \cos\alpha} \qquad (8)$$

For several typical metal braids the attenuation factor $\exp(-\tau)$ has been calculated to be between 0.08 and 0.21. Hence, the so-called “chimney” effect reduces the magnitude of the hole inductance considerably.

As follows from equations (5) and (6) the hole inductance increases linearly by the value of the magnetic polarizability $m$ of the rhombic hole. For small apertures in zero-thickness walls the magnetic polarizability has been discussed in Ref [7] and [8]. In these papers it was shown that the symmetric magnetic polarizability $\overline{\overline{m}}$ dyadic can be written as

$$\bar{\bar{m}} = S^{3/2}(\nu_{mx}\bar{u}_x\bar{u}_x + \nu_{my}\bar{u}_y\bar{u}_y) \qquad (9)$$

where $S$ the surface of the aperture, and $\nu_{mx}$ and $\nu_{my}$ are dimensionless normalized magnetic polarizabilities along the principal axes of the dyadic. Notice that the magnetic polarizability $\bar{\bar{m}}$ dyadic has typical length scale cubed. Furthermore, it was shown in Ref [8] that the dimensionless magnetic polarizabilities of elliptical and rhombic apertures are almost equal. For elliptical apertures the dimensionless magnetic polarizabilities are given by

$$\nu_{mx} = \frac{2}{3\sqrt{\pi}}\left(\frac{l}{w}\right)^{3/2}\left(\frac{e^2}{K(e)-E(e)}\right) \qquad (10)$$

and

$$\nu_{my} = \frac{2}{3\sqrt{\pi}}\left(\frac{l}{w}\right)^{3/2}\left(\frac{(1-e^2)e^2}{E(e)-(1-e^2)K(e)}\right) \qquad (11)$$

In the above formulas $e$ is the eccentricity of the ellipse, $e=\sqrt{1-(w/l)^2}$ (with $l$ major axis and $w$ the minor axis), and $K(e)$ and $E(e)$ are the complete elliptical integrals of the first and second kind.

The magnetic polarizabilities of the rhombic apertures of the metal braids follow now from equations (9) to (11). For weave angles $\alpha$ larger than 45 degrees the magnetic fields due to a current along the axis are parallel to the *x*-axis. For this case, the magnetic polarizability reads

$$m_x = S_r^{3/2}\nu_{mx} \qquad (12)$$

with $S_r$ the surface of the rhombic aperture,

$$S_r = lw/2 \qquad (13)$$

For weave angles $\alpha$ smaller than 45 degrees the magnetic fields due to a current along the axis are parallel to the *y*-axis. For this case, the magnetic polarizability reads

$$m_y = S_r^{3/2}\nu_{my} \qquad (14)$$

However, in Ref [1] and [3] the magnetic polarizabilities of rhombic apertures are approximated by magnetic polarizabilities of equivalent elliptical apertures. More exactly, in Ref [1] and [3] the surface of an elliptical hole with area

$$S_e = \pi lw/4 \qquad (15)$$

is applied in equation (9). As a consequence, the values of the magnetic polarizabilities are overestimated in Ref [1] and [3]. The surfaces of the rhombic apertures should be used in equations (12) and (14), and not the surface areas of the elliptical holes. Hence, with reference to equations (12) and (14) the overestimate factor amounts

$$\Gamma = (S_r/S_e)^{3/2} = (2/\pi)^{3/2} = 0.5079 \qquad (16)$$

As a consequence, the hole inductance formulas of Vance by equation (5) and Kley by equation (6) should be reduced by a factor $\Gamma = 0.5079$. Thus, the improved formula for the hole inductance becomes

$$M_h = 0.875\frac{\mu m}{2\pi^2 D_m^2}\Gamma e^{-\tau} \qquad (17)$$

## V. BRAID INDUCTANCE

The modeling of the braid inductance has been discussed in references [4], [5] and [6]. The braid inductance is caused by magnetic flux linkage between the inner and outer braid layers due to the woven structure of the braid. The principle of this flux linkage is shown in Figure 4. These figures show the representation of the flux area between the spindles of the braid.

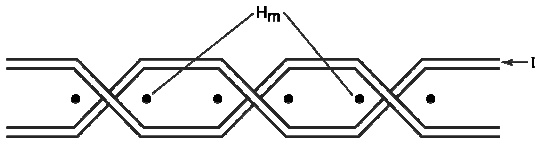


Figure 4 Representation of flux area in Tyni's model

The area in Figure 4 was considered by [4] to derive the following formula for the braid inductance per unit length,

$$M_b = -\mu\frac{d}{4\pi D_m}\frac{\hat{h}}{d}(1-\tan^2\alpha) \qquad (18)$$

The average height $\hat{h}$ in formula (18) plays a crucial role in determining the values of the braid inductance $M_b$. It appears to be rather difficult to determine correct values for $\hat{h}$. With reference to [4] $\hat{h} \simeq d$ for dense braids. In loose braids, the layers can be close to each other and the value of $\hat{h}$ is smaller.

Kley [3]applies the following approximate formula

$$M_b = -\mu\frac{d}{4\pi D_m}\frac{0.22}{F\cos\alpha}\cos(2k_1\alpha) \qquad (19)$$

where

$$k_1 = \pi/4\left[\frac{2}{2}F\cos\alpha + \frac{\pi}{10}\right]^{-1}$$

The main difference between the braid inductance of [3] and [4] is the dependence on the weave angle $\alpha$. By equation (18) Tyni [4] supposes that the braid inductance decreases by

$$m_T^{\alpha} = (\hat{h}/d)(1-\tan^2\alpha) \qquad (20)$$

for increasing weave angles, while Kley assumes a decrease by a factor (see equation (19))

$$m_K^\alpha = \frac{0.22}{F\cos\alpha}\cos(2k_1\alpha) \qquad (21)$$

The values of $m_T^\alpha$ and $m_K^\alpha$ are displayed in Figure 5 for $\hat{h} = d$ and for fill factor $F$=0.8. Inspection of this figure reveals that Kley's model (see equation (19)) reduces the effect of the braid inductance much more than Tyni's model (see equation (18)) for weave angles less than 45 degrees. When we assume $\hat{h} = d/4$, then the values of $m_T^\alpha$ have to be reduced by a factor 0.25. Then, a much closer correlation is obtained for the factors $m_T^\alpha$ and $m_K^\alpha$.

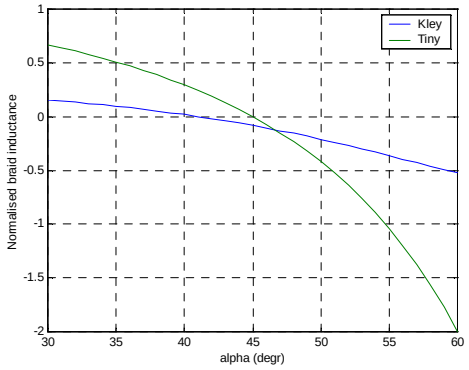


Figure 5 Calculation of $m_T^\alpha$ and $m_K^\alpha$ for weave angles between 30 and 60 degrees (fill factor F=0.8, $\hat{h} = d$ )

It can be concluded that the average height $\hat{h}$ in formula (18) is an important parameter that strongly determines the magnitude of the braid inductance. Tyni proposes the following formula for the average height,

$$\hat{h} = \frac{2d}{1+b/d} \qquad (22)$$

with $b/d = N(1-F)/F$. For dense braids $F$ is about 0.8 and typical values for the number of wires per carrier are $N$=5 to $N$=8. With these values $b/d$ is between 1.25 and 2. It follows that the average height $\hat{h}$ in formula (22) ranges from 0.67$d$ to 0.89$d$. Notice that these values are much larger than $d$/4, which was required to achieve a close resemblance between the factors $m_T^\alpha$ and $m_K^\alpha$. As a consequence, the proposition is that the braid inductance according to Tyni (as described by equations (18) and (22)) will yield higher values than Kley's model (given by equations (19)).

Notice that for weave angles $\alpha < 45^o$ the hole inductance and braid inductance oppose each other. Furthermore, in case the braid inductance is dominant over the hole inductance then $(M_h + M_b) < 0$, which will result in polarity change of the transfer impedance.

## VI. Computational Tools

The transfer impedance will be calculated by three different tools. These tools are:

1. Vance's model, defined by equations (1), (2) and (5).
2. Kley's model, defined by equations (1), (2), (6) and (19)
3. Our improved model, defined by equations (1), (2), (17), (18) and (19). This model will be referred as Beatrics in the following sections.

## VII. Results

The braid inductances according to formulas (18) and (19) have been computed for 19 different braid samples. The results are displayed in Figure 6, indicated by BTiny and BKley, respectively. Figure 6 contains also the values of the hole inductances by Vance (5), Kley (6) and the improvement by (17), which are indicated by MVance, MKley and MBea respectively in Figure 6. This figure shows that braid inductance dominates over hole inductance for most samples, and that braid inductance according to Tyni ((18) and (22)) yields a significant larger contribution than Kley's model (equation (19)).

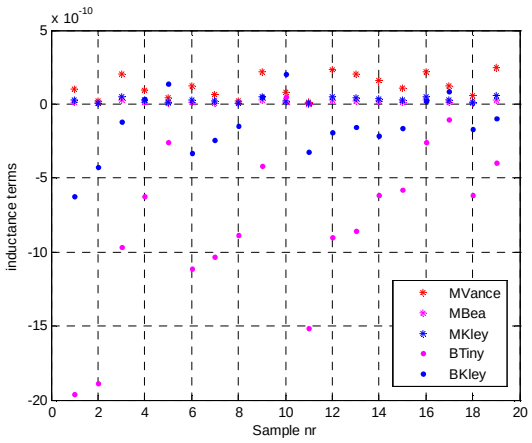


Figure 6 Values of hole inductances by Vance (5), Kley (6), Bea (17) and braid inductances by Tyni (18) and Kley (19).

Inspection of Figure 6 reveals that the contribution of hole inductance is small (in comparison to braid inductance) for samples 2, 8 and 11. The calculated absolute values of transfer impedances of sample 8 are displayed in Figure 7, and compared with the outcome of measurements. The geometrical data of sample 8 are: D=6 mm, d=202 µm, N=7, C=24 and α=38.6 degrees. Figure 7 reveals a fair comparison between the outcome of the Beatrics tool and the measurements. Notice the Beatrics tool uses the braid inductance according to Tyni (18) with the average height defined by (22). Hence, for this sample the average height by (22) is appropriate. Furthermore, Figure 7 shows that the tools of Vance and Kley underestimate the transfer impedance due to short of braid inductance. The phases of the calculated transfer impedances of sample 8 are displayed in Figure 8.

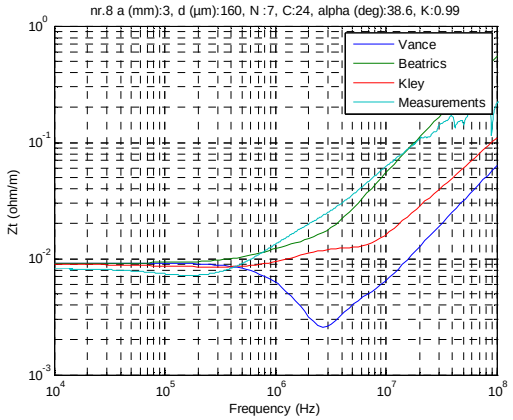


Figure 7 Transfer impedance of sample 8; Comparison of Vance, Beatrics and Kley tools with measurements

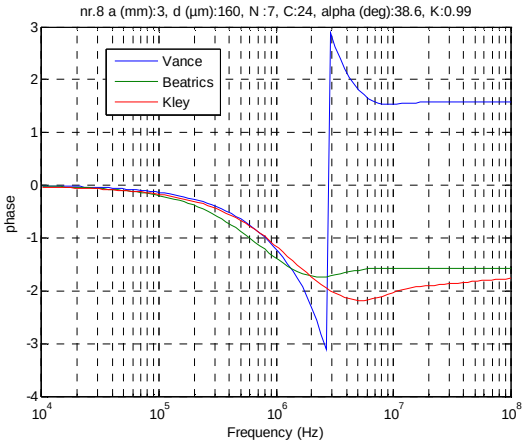


Figure 8 Phase of transfer impedances of sample 8

Observe from Figure 8 that the phase behavior is different for the outcome of Vance's tool and the other ones. Vance's tool only contains a contribution from hole inductance, which is positive for all frequencies. In the other tools the braid inductance is dominant over the hole inductance (see Figure **6**). For this sample $(M_h + M_b) < 0$ , which results in a polarity change of the transfer impedance.

Inspection of Figure 6 shows that samples 8 and 12 have similar values of braid inductance, while the values of hole inductance are different. For sample 12 the contribution of hole inductance is more substantial, at least of Vance's tool. The geometrical data of sample 12 are: D=8 mm, d=202 μm, N=5, C=32 and α=35 degrees. The calculated and measured transfer impedances of sample 12 are displayed in Figure 9. Observe from the measured data that braid inductance is less significant for this sample. It is obvious that the contribution of braid inductance of the Beatrics tool is too high. Notice that the braid inductance increases linearly by the average height $\hat{h}$ by equation (18). Formula (22) predicts an average height of 0.73d for sample 12, which is too large. In **Figure 10** the average height has been varied between 0.1*d* and 1.0*d*. From this figure it can be concluded that an average height of 0.25 *d* would have been appropriate for this sample, because for higher frequencies the measured data is contained between the curves of 0.2*d* and 0.3*d*.

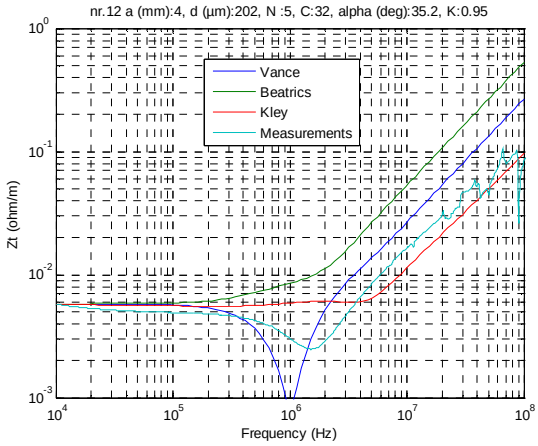


Figure 9 Transfer impedance of sample 8; Comparison of Vance, Beatrics and Kley tools with measurements

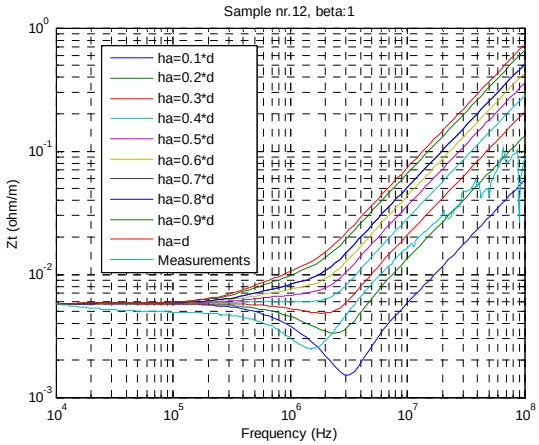


Figure 10 Transfer impedance of sample 8 as calculated by Beatrics tool, where the average height $\hat{h}$ is varied between 0.1*d* and 1.0*d*.

The main difference between sample 8 and sample 12 is the optical coverage. For sample 8 the optical coverage is 0.99, while for sample 12 it is 0.95. It could be that braids with lower optical coverage are more loose, so that the spindles of the braid are more close, which will result in a lower average height between the spindles. More knowledge of the manufacturing process of metal braids could also contribute to explaining differences in heights between spindles of braids.

## VIII. CONCLUSIONS

In this paper analytical models for the calculation of transfer impedance for metal braids have been considered. These models contain two components, one part ( $Z_d$ ) representing diffusion of electromagnetic energy through the metal braid, and a second part ( $j\omega M$ ) representing leakage

of magnetic fields through the braid. The diffusion component $Z_d$ of the metal braid is governed by the DC resistance of the metal braid and diffusion of waves through the wall of the cylindrical braid. The inductance $M$ in equation (1) is the superposition of the hole inductance $M_h$, braid inductance $M_b$ and skin inductance $M_s$. The diffusion component $Z_d$ is dominant at low frequencies; the hole inductance and braid inductance dominate at high frequencies. The skin inductance only yields a small contribution in the central region (between low and high frequencies).

The analytical models of Vance (see ref [1]and [2]) and Kley [3] have been applied to a set of 19 sample braids. The diffusion component $Z_d$ is calculated carefully by the models of Vance and Kley. However, the effects of inductance are not predicted accurately enough by these models. The transfer impedance of most samples is dominated by effects of braid inductance $M_b$. The model of Vance neglects braid inductance at all. The braid inductance model of Kley (see equation (19)) contains semi-empirical parameters which have been adjusted by Kley to measured data of a set of optimized braids. The application of this model to the set of 19 samples as considered in this paper does not provide a fair correlation between simulations and NLR's measurements. A more detailed modeling of braid inductance and detailed knowledge of cross sections of metal braids are required to resolve the real contribution of braid inductance.

Acknowledgment

The work described in this paper and the research leading to these results has received funding from the European Community's Seventh Framework Programme FP7/2007-2013, under grant agreement no. 205294, HIRF SE project.

## REFERENCES

[1] Vance, E.F., Shielding effectiveness of braided-wire shields, Interaction Note 172, Stanford Research Institute, April 1974.

[2] Vance, E.F., Shielding effectiveness of braided-wire shields, IEEE Transactions on, Electromagnetic Compatibility, Vol.17, no. 2, May 1975, 71-77

[3] Kley, T., Optimized Single-Braided Cable Shields, IEEE Trans. On EMC, Vol. 35, No. 1, February , 1-9, , 1993

[4] Tyni, M.; The Transfer Impedance of Coaxial Cables with Braided Outer Conductor, FV. Nauk, Inst. Telekomum Akust. Politech Wroclaw, Ser. Konfi, pp. 410-419, 1975.

[5] Sali, S.; An improved model for the transfer impedance calculations of braided coaxial cables, IEEE Trans. on Electromagnetic Compatibility, Vol. 33, pp. 139-143, 1991.

[6] Benson, F.A.; Cudd, P.A.; Tealby, J.M.; Leakage from Coaxial Cables, IEE Proceedings A, Vol. 139, pp. 285-303, 1992.

[7] De Smedt, R.; Van Bladel, J.; Magnetic polarizability of some small apertures, IEEE Transactions on Antennas and Propagation, Issue Date: Sep 1980 Volume: 28 Issue:5, page(s): 703 - 707

[8] F. De Meulenaere and J. Van Bladel; Polarizability of some small apertures, IEEE Trans. Antennas Propagat., vol. AP-25, pp. 198, 1977.

[9] Tiedemann, R.; Current Flow in Coaxial Braided Cable Shields, IEEE Trans. on Electromagnetic Compatibility, Vol. 45, pp. 531-537, 2003.

[10] R. E. Collin, Field Theory of Guided Waves., 1960 :McGraw-Hill

[11] H. Kaden, Wirbelströme und Schirmung in der Nachrichtentechnik, 1959, new edition 2006, Springer Verlag

[12] Butler, C. ; Rahmat-Samii, Y. ; Mittra, R., Electromagnetic penetration through apertures in conducting surfaces, IEEE Trans. Antennas Propagat., vol. AP-26, pp. 82-93,1978

[13] Otin, R.; Verpoorte, J.; Schippers, H; A Finite Element Model for the Computation of the Transfer Impedance of Cable shields, Submitted for publication to IEEE Trans. on Electromagnetic Compatibility